Jens Ekengren

Estimating inclusion content in high performance steels

Jens Ekengren

Estimating inclusion content in high performance steels

Abstract

Non-metallic inclusions in steel pose a major problem for the fatigue resistance, especially regarding fatigue at very long lives corresponding to low cyclic stress levels, as well as being detrimental to material toughness and polishability.

The largest inclusions are quite rare, which makes conventional detection methods time-consuming if reliable results are to be obtained. Based on surface scanning using light or electron microscopes, these methods provide results that have to be converted to reflect the statistical volume distribution of inclusions.

Very high cycle fatigue (in the order of 10^9 cycles or more) using ultrasonic fatigue at 20 kHz has been found efficient at finding the largest inclusions in volumes of about 300 mm^3 per specimen. The inclusions found at the fatigue initiation site can then been used to estimate the distribution of large inclusions using extreme value statistics.

In this work, a new method for estimating the volume distribution of large inclusions is presented. The method is based on the extreme value distribution of inclusions found on fatigue fracture surfaces. Further, a ranking variable based on the volume distribution is proposed and tested by comparing results from fatigue fractography and area scanning methods to the fatigue strength at 10^9 cycles for a number of batches from two high performance steels.

In addition the extreme value distributions of fatigue initiating inclusions in six high performance steels, produced by different routes, are presented. It is shown that all modes of the Generalized Extreme Values distribution can be found in different materials. This result shows that the assumption of mode I distribution, also known as Gumbel or Largest Extreme Value distribution, must be substantiated.

ACKNOWLEDGEMENTS

List of enclosed papers

This licentiate thesis comprises the following papers, which will be referred to by their roman numerals:

Paper I
J. Ekengren, V. Kazymyrovych, C. Burman, J. Bergström, "*Relating Gigacycle Fatigue to Other Methods in Evaluating the Inclusion Distribution of a H13 Tool Steel*", in **Fourth International Conference on Very High Cycle Fatigue (Book and CD-ROM)** Edited by: John E. Allison, J. Wayne Jones, James M. Larsen, and Robert O. Ritchie. ISBN 978-0-87339-704-9.

Paper II
J. Ekengren, J. Bergström, "*Detecting large inclusions in steels: evaluating methods*", in manuscript.

Paper III
J. Ekengren, J. Bergström, "*Extreme value distributions of inclusions in six steels*", in manuscript.

Literature Review
J. Ekengren, "*Finding non-metallic inclusions in clean steel*", Karlstad University Studies, ISBN 978-91-7063-208-2

Contents

1 Introduction

Non-metallic inclusions are a type of defects present in steel that severely effect properties like polishability, ductility and fatigue strength. Because of the decreasing number of inclusions with increasing size, the different size intervals pose different problems. With respect to polishability, the large number of inclusions smaller than, say, size I in Fig. 1 are more harmful than the larger but simultaneously rarer inclusions simply by being more frequently occurring. On the other hand, at low stress levels critical cracks that
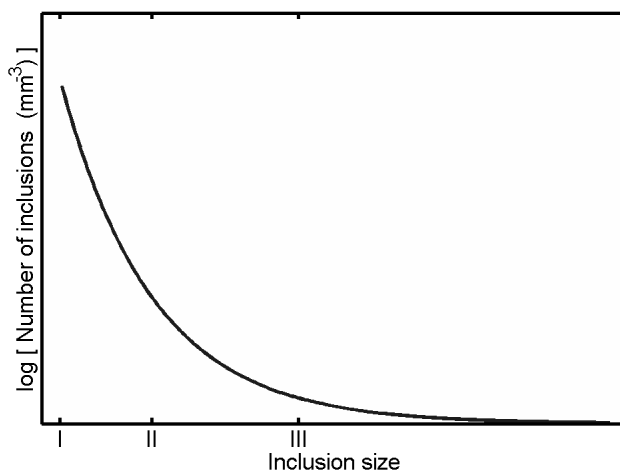

Figure 1: *Schematic figure of inclusion density as a function of inclusion size.*

can lead to failure within a product's lifetime, will most likely grow at the very largest inclusions, larger than size III. These inclusions are rare and it is difficult to correctly estimate their occurrence density. At intermediate fatigue stress levels inclusions of sizes around II compete with surface flaws as the crack initiation points.

In this work methods for determining the statistical distribution of non-metallic inclusions in steel are presented. Examples of the methods used are area scanning, using light or electron microscope, volume scanning using ultrasound immersion tank and fatigue testing. The focus is on using fatigue to 10^9 cycles as the means of detection and statistics of extreme values to evaluate the detected inclusion distributions.

1.1 Non-metallic inclusions

Non-metallic inclusions are chemical compounds consisting of at least one non-metallic component, such as sulphur or oxygen. In high strength steels they are an unwanted but largely unavoidable phase caused by the content of oxidising agents in the steel melt due to the raw material or introduced during melting.

The composition of the inclusion is an inducator to its origin, for example can an inclusion containing sulphur usually be traced to the sulphur content of the raw material whereas aluminium oxides may form during deoxidising using added aluminium during ladle treatment. Inclusions are detrimental to the fatigue properties, as will be discussed throughout this work, but also adversely effect properties like polishability, corrosion resistance and ductility [1].

Increasing use of high strength steels, for example in automotive engineering applications, places tougher demands on the tool steels used in manufacturing. One of those requirements is improved cleanliness, particularly as measured by the content of large inclusions.

1.2 Properties of tool steels

Tool steels constitute a very small part of the total tonnage of steel manufactured, but their properties make them very important. Tool steels are generally harder than construction grades and can usually withstand much larger loads before failing. The high hardness is obtained via matrix hardening due to increased lattice distortion and via precipitation of small carbides caused by the alloying elements. Both of these mechanisms work by hindering dislocation movement.

Some tool steels are designed for hot working and can endure severe loads at high temperatures. Others are designed to be highly resistant to abrasive wear or to have a minimal distortion during hardening while providing sufficient hardness. These properties are attained by alloying the iron-carbon base with different elements such as vanadium, tungsten, chromium or silicon. The demands placed on alloying control both in terms of concentration and of absence of segregation make production of tool steel challenging. Precise control of alloying elements and removal of contaminations are important to ensure high quality products. The molten steel can be solidified using routes such as ingot casting, spray forming or powder metallurgy. Cast ingots can then be remelted using methods as electroslag remelting (ESR) or vacuum induction melting/vacuum arc remelting (VIM/VAR). Extensive hot working after solidfication or remelting is also common to produce a homogeneous structure consisting of small grains, which further improves the properties.

1.3 Fatigue background

Almost all objects around us are subjected to varying loads during their life. Some are loaded beyond their capability and fail quickly due to severe plastic deformation and cracking. Others are subjected to repeated loads where each load cycle is not enough to cause immediate failure, but where accumulated damage causes eventual failure. This mode of failure is called fatigue and is most common in metallic materials. The first mentions of the concept were in the early 19th century, and one name that is connected to pioneering research in metal fatigue is that of August Wöhler, engineer at a German railroad company [2].

As the number of load cycles increases, the maximum allowable stress decreases, as is shown in a $S - N$ diagram such as Fig. 2. For steel, there usually is a plateau starting around 10^5-10^6 cycles and reaching to about 10^7-10^8 cycles, where the maximum allowable stress does not seem to decrease.
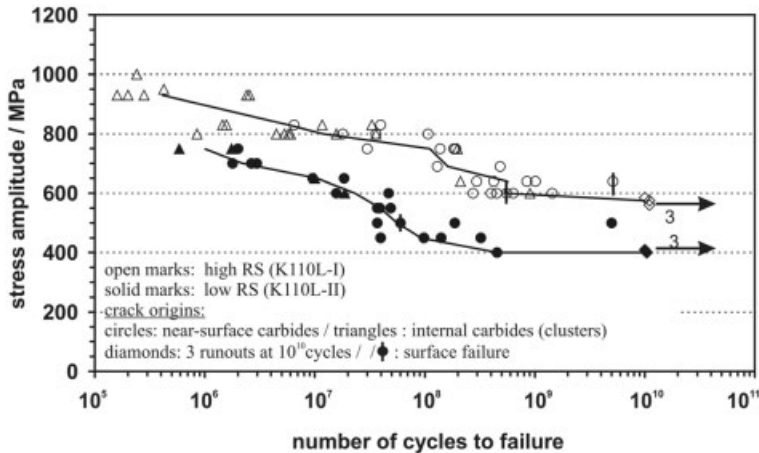

Figure 2: *Diagram presenting stress level vs number of cycles for a high-chromium tool steel with different residual surface stresses. Image from [3]*

This may have led to a belief that there is a minimal stress that casues damage. This has been disputed with evidence from testing to large numbers of cycles [4], as a second decline begins around 10^7 cycles. The plateau and second decline are usually connected with a change in fatigue crack initiation. During low cycle fatigue with large stress amplitudes, the cracks are usually initiated at defects along the surface of the material. As the stresses decrease and more cycles are needed to produce critically sized cracks, cracks are rather started at interior defects such as non-metallic inclusions, unbroken primary carbides or porosities.

2 Finding inclusions in steel

In order to evaluate the cleanliness and risk of failure in fatigue, one needs to find the distribution of inclusions. Several methods exist, which can be classified according to a number of different criteria:

- **Area scanning methods** where a polished surface is scanned using light optical or scanning electron microscope, and the sizes of found inclusions are analyzed. Large scanning areas are needed to reduce statistical uncertainty for large inclusions [5]. If scanning electron microscopes are used, additional information about inclusion chemistry can be obtained. Another type of method analyzes the light emitted from

spark discharges along the surface. Area scanning methods are most efficient in finding the small but common inclusions in the left end of fig. 1.

- **Non-destructive methods** such as ultrasonic defect echo finder in which a ultrasonic wave is sent from a moving transmitter at the surface, is reflected at defects and then picked up by a detector. Smaller inclusions can be found and mapped by cutting a plate and scanning this using higher frequencies. Non-destructive methods are better at locating larger inclusions, but may have problems with correctly estimating their size.

- **Inclusion enrichment methods** such as chemical dissolution or cold crucible remelting. In the first family, the matrix is dissolved leaving the inclusions behind and their distribution can be estimated [6] and in the second, inclusions float to the surface of melted material and can be counted to evaluate the distribution. Inclusion enrichment methods can, theoretically, find all inclusions within a piece of steel, but due to the number of small inclusions there is a risk that they receive the main attention.

- **Fatigue** can be an efficient way of finding inclusions, as cracks primarily grow from microstructural defects. As explained by Nordberg, lowering stresses and correspondingly increasing the number of load cycles raise the modal point of the size distribution of initiating inclusions [7]. Fatigue can find very large inclusions, but is usually limited to finding only one of the largest inclusions within the stressed material.

Each of these methods have their advantages and disadvantages. For example, acid used in chemical dissolution methods may also dissolve sulphide inclusions [6]. If porosities are present in the material, they would cause fatigue if sufficiently large, but would not show up using methods based on chemical composition.

The size distributions obtained by the different methods also differ in terms of if they are based on area or volume, which may makes comparison of results difficult.

One way of translating area measurements to volume distributions is by assuming a detection depth equal to the average size of the found inclusions and setting the effectively scanned volume to $V = A \cdot h$. Another way involves calculating the probabilities of an inclusion cross section area being the result of cutting an inclusion of a certain size with a plane.

3 Models relating inclusions and fatigue performance

As defects are present in most, or even all, commercially available steels it is important to relate their sizes to behaviour in fatigue. Several models try to describe the relation between the size of defects present in the material and the fatigue strength, the stress level at which failure occurs in half of the specimens before a certain number of cycles.

3.1 Kitagawa-Takahashi model

The behaviour of a cyclically stressed material with existing defects depends heavily on the size of the defects. If large cracks are present in a stressed volume, the stress level needed for critical crack growth can be modelled with Linear-Elastic Fracture Mechanics (LEFM) in which the stress intensity range ΔK is calculated as a function of crack size, crack shape, position in the specimen and stress level σ, such as

$$\Delta K \approx \frac{2}{\pi} \Delta \sigma \sqrt{\pi a} \tag{1}$$

for an internal circular crack [8].

On the other hand, when no large defects are present fatigue cracks may be initiated at intrinsic material faults, such as grain boundary segregation or slip bands formed during loading. This lower limit is roughly corresponding to the size of microstructural features, for steel mainly the grain size. For sizes below this the fatigue strength is constant no matter the actual size, according to the model illustrated in Fig. 3, depicting the critical stress levels for a medium carbon steel [9]. The Kitagawa-Takahashi model is valid for several materials, including human dentin [10]. Above the critical stress level/defect size
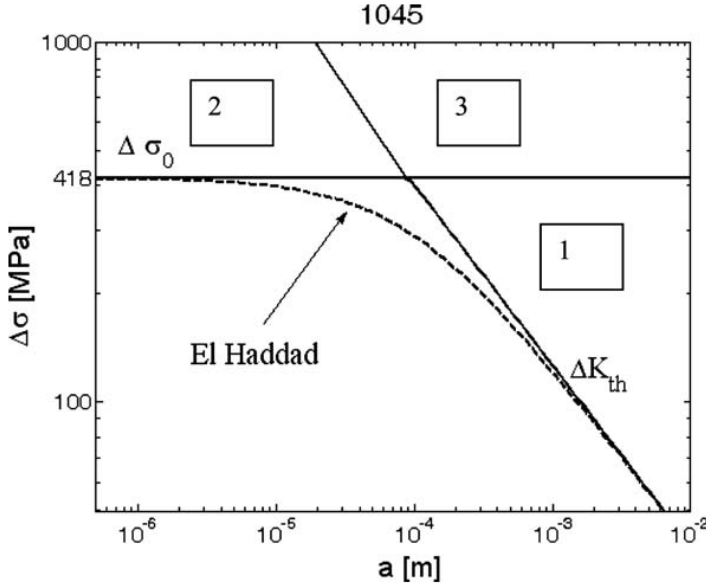
Figure 3: *Kitagawa-Takahashi diagram for a medium carbon steel. From [9].*

line, failure is expected to occur before a certain number of load cycles, whereas below, failure is not expected. In the transition region, close to where the two critical stress/size lines intersect, the critical stress/size falls below the lines. The effective limit in these cases can be estimated by, for example, the Murakami $\sqrt{(Area)}$ or the El Haddad a_0 models.

3.1.1 Murakami $\sqrt{(Area)}$ and El Haddad model

The Murakami $\sqrt{(Area)}$ model approximates the critical conditions for the transition region with a straight line, given by the semi-empirical expression

$$\sigma_w = K \left(HV + 120\right) \sqrt{area}^{-1/6} \left[(1 - R)/2\right]^\alpha \tag{2}$$

with K = 1.43 for surface defects and =1.56 for interior defects. HV is the material's Vickers hardness and $\alpha = 0.226 + HV \cdot 10^{-4}$.

The El Haddad model instead uses the same equation for the stress intensity factor as the LEFM, but replaces the actual crack size a with an effective size $a + a_0$, where a_0 is given by the horizontal asymptote given in Fig. 3, defining an intrinsic defects limit as

$$a_0 = \left(\frac{\Delta K_{TH}}{Y \Delta \sigma_{fat}}\right)^2 \frac{1}{\pi} \tag{3}$$

where ΔK_{TH} is the threshold value for critical growth of large cracks, Y is the correction factor depending on crack shape and σ_{fat} is the fatigue strength with no defects present [10].

3.2 Nordberg model

In [7] the risk of a test specimen with a stressed volume V failing due to an inclusion in size class J at a stress level σ is written as

$$
\begin{aligned}
P(\sigma, J) \quad = \quad & \left[\prod_{I=J+1}^{\infty} \exp(-N(I) \cdot V)\right] \times \left[1 - \exp(-N(J) \cdot V)\right] \times \\
& \times \frac{1}{\sqrt{2\pi}} \int_{-\infty}^{X} \exp(-u^{-2}/2) \mathrm{d}u
\end{aligned}
\tag{4}
$$

where $N(i)$ is the density of inclusions in size class i. The probability is the product of three factors,

- The probability of not having failed due to the existence of larger defects $\times$

- The probability to find one or more inclusions belonging to size class J within the specimen volume $\times$

- The probability to fail at this stress due to an inclusion of this size.

The probability to fail before $2 \cdot 10^6$ cycles is considered to be a normal distribution given by the approximative fatigue strength, given as $\sigma_u = \dfrac{\alpha R_m}{1 - (K_T - 1) / (1 + 2a/D)}$,

$a = 0.025 \left(\frac{2070}{R_m} \right)^{1.8}$ and standard deviation S, incorporated via the upper integration limit $X = \frac{\sigma - \sigma_u}{S}$. If inclusions are assumed to be approximately spherical, $K_T = 2$.

Underlying assumptions are that failure may occur as long as at least one inclusion is present, and that failure occurs only due to the biggest inclusion (if several are present) or not at all.

4 Statistics of extreme values

When one wants to analyze some rare events, such as flood levels or peak temperatures, ordinary statistical methods fail to properly describe their distribution. This is because most standard statistics deal with the "normal events" instead of those at the ends of the distribution. Many of these methods tend to lower the influence of precisely those rare events we are interested in. A more appropriate method for these cases is extreme value statistics which deals with those events on the far ends of the measurements that might be considered outliers under normal statistical analysis.

Another example of extreme values, of great interest when discussing the mechanical properties of tool steel, is the size of the largest inclusion found in a stressed volume.

For all these examples, the probability of the maximum being over a certain value z can be described by a mode of the Generalized Extreme Value (GEV) distribution [11]

$$G(z) = \exp \left\{ - \left[1 + \xi \left(\frac{z - \mu}{\sigma} \right) \right]^{-1/\xi} \right\} \tag{5}$$

with three parameters for location, scale and shape, μ, σ and ξ. As $\xi \to 0$ the distribution goes towards a Gumbel distribution,

$$G_1(z) = \exp \left\{ -\exp \left[-\frac{z - \mu}{\sigma} \right] \right\} \tag{6}$$

In Fig. 4, the cumulative distribution for the GEV has been plotted for three different values of ξ, using constant values for μ and σ.

The expected largest extreme value is largely dependent on the shape parameter ξ, with a finite maximum for $\xi < 0$. In Fig. 4 this can be seen as $-\log(-\log[G(z)])$ tends to infinity at $z = 80$. For non-negative values of ξ, the distribution function decreases steadily; however, larger values of ξ lead to slower declines. The Gumbel family has a exponentially decaying density with a rate that depends on the scale parameter σ.

If not only the largest value within each sample is measured, but rather all values above some threshold, methods in the Peaks-Over-Threshold (POT) family might be better to as they use more of the available information. The analogue to the maximal values' Generalized Extreme Values distribution when using POT is the Generalized Pareto Distribution
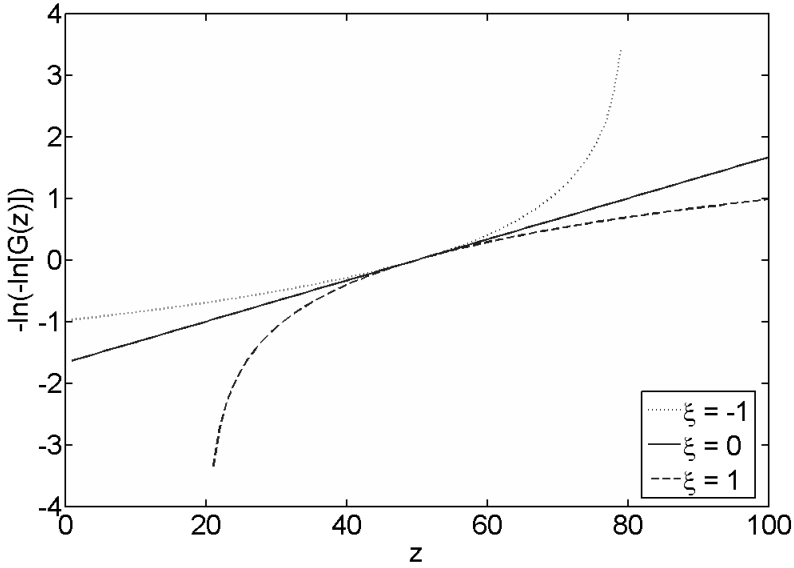
Figure 4: *The three different apperances of the GEV distributions. σ = 30, μ = 50 and ξ as indicated.*

(GPD). In fact the shape parameter is the same for both when calculated from the same observations [11].

4.1 Estimating inclusion distribution from extreme values

It may be assumed that the fracture initiates at the largest inclusion within the stressed volume and if no fracture occurs one can assume that no inclusion above a critical size is present.

The critical size may be calculated from the stress level at which the non-fractured specimens were tested and this information may be used to evaluate the maximal size of inclusions present in those specimens. By combining the sizes found at fracture surfaces and the largest inclusions expected to be found in the non-broken, censored, specimens additional estimation about the total inclusion distribution can be achieved [12].

Extreme value statistics can be employed to estimate the largest inclusion on areas scanned using microscope and this size may then be used to calculate the risk of failure during fatigue tests or in products in real use.

When the density of large inclusions has been estimated using area scanned surface samples, the result can be roughly transformed to volume distribution by assuming a "scanning depth" comparable to the linear size of inclusions, that is $V_{scan} = A_{scan} \cdot h$, where

h is the average size of inclusions.

If large inclusions, that is inclusions larger than a certain threshold u_0, are randomly distributed on a set of measurement surfaces, each of area A, and if the distribution of sizes above the threshold is exponentially decaying, the distribution of the largest inclusion of each surface can be shown to follow a Gumbel distribution [13] with parameters

$$\mu = u_0 + \alpha \log(A\lambda(u_0)) \tag{7}$$
$$\sigma = \alpha \tag{8}$$

where $\lambda(u_0)$ is the density of inclusions larger than u_0 and α is the parameter of the exponential distribution.

5 Experimental methods and results

A number of steels, with different chemical composition and produced by different process routes (see Table 1), have been tested in an ultrasonic resonance fatigue rig, working at a frequency of 20 kHz. By use of pre-stress the ratio between maximum and minimum stress during the stress cycle was kept at $R = 0.1$. Compressed air was used to cool the waist of specimens during testing. Specimens were manufactured from hot-worked ma-

Table 1: *Material label, route label, material hardness and number of batches for the six materials.*

Material	Process route	Hardness (HV)	No of batches
A	I	430-470	5
B	I	465-495	5
C	II	485-505	3
D	III	705-715	5
E	III	660	1
F	IV	430	1

terial and taken out so the length axis was parallel to the short tranverse axis of the steel billet and machined to dimensions shown in Fig. 5. Final grinding and polishing was performed after heat treatment. Fatigue fracture surfaces were examined using a scanning electron microscope with energy dispersive spectroscopy capabilities and inclusion size, position and approximate chemical composition were recorded. Two steels, denominated A and D in table 1, were also investigated using light and scanning electron microscope.

5.1 Extreme value distribution to volume distribution

The results from area scanning methods and ultrasonic immersion tank measurements were compared to results from fractography on specimens tested in ultrasonic fatigue to
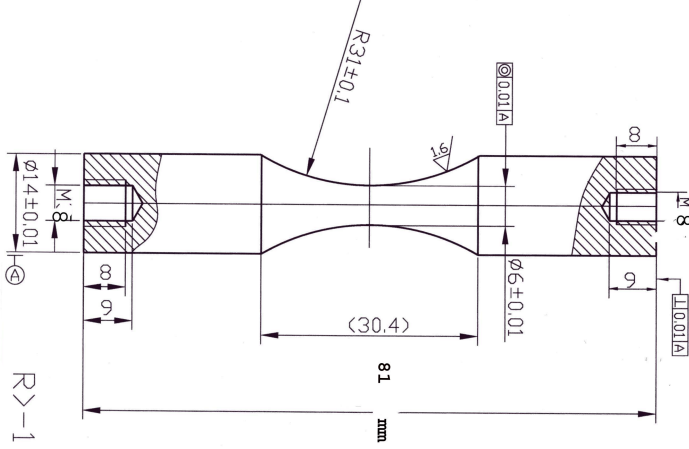
Figure 5: *The ultrasonic resonance fatigue specimen.*

10^9 cycles. The area inclusion distribution was estimated using light optical microscopy and scanning electron microscopy.

The use of extreme value statistics based on the sizes of fatigue initiating inclusions and subsequent inference to the volume densities of large inclusions suggested that the distribution of large defects found during fatigue differs from that of inclusions detected using optical and scanning electron microscopy.

The approach from section 4.1 can be directly applied to volumes, and when reversed it provides a link between the inclusions found on fracture surfaces and the underlying distribution of large inclusions. If the critical threshold for fatigue crack growth is assumed to be as large as the smallest inclusion found at the fracture initiation, this size can be used as the threshold u_0.

In this way, the distribution of large inclusions can be approximated from the defects found at fatigue fracture initiation sites under the assumptions that

- inclusions larger than the threshold are randomly distributed,

- the density of inclusion size of these inclusions is decaying exponentially, and

- the inclusions found at fatigue fracture surfaces follow a Gumbel distribution.

The expected density of large inclusions per unit volume is then given by

$$N_V(u_0) = \exp\left[\left(\frac{(\hat{\mu} - u_0)}{\hat{\sigma}}\right)/V\right] \tag{9}$$

10

where u_0 is the smallest inclusion found at fatigue fracture surfaces, $\alpha = \hat{\sigma}$ is the scale parameter estimated from the Gumbel distribution, and V being the stressed volume.

In the current research $V = 2 \cdot V_1$, where V_1 is the critically stressed volume of one fatigue specimen, is used to compensate for using only that half of specimens that broke during fatigue testing.

$N_V(z)$, the accumulated density of inclusions larger than $z > s_0$, is calculated as

$$N_V(z) = N_V(s_0) \cdot \exp\left(-\frac{s_0 - z}{\hat{\sigma}}\right) \tag{10}$$

being the estimated number of inclusions larger than s_0 times the probability of the individual inclusions also being larger than z. In Fig. 6 the volume distributions of inclusions, as estimated by all four methods are shown. The end of the graphs for the different methods show the sizes of inclusions found, emphasising the differences in effective detection capability.
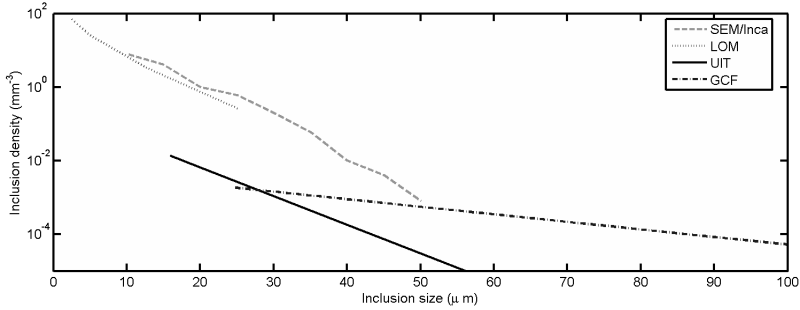

Figure 6: *Volume distribution of inclusions in an H13 steel, estimated using two area scanning methods, ultrasound immersion tank and gigacycle fatigue fractography.*

This work was presented at the 4th international conference on Very High Cycle Fatigue (VHCF-4).

5.2 Comparing detection methods

In this work two high performance steels were compared with respect to fatigue strength at 10^9 cycles and the calculated sizes at which approximately half of the specimen would contain a defect of this size or bigger, given as

$$N_V(S_x) = \int_{S_x}^{\infty} g_v(s) \mathrm{d}s \tag{11}$$

calculated according to results from

LOM area densities obtained from investigations with light optical microscope

SEM area densities from automatic scanning electron microscope (used for one batch of each material) or

GCF fractography of specimens used in ultrasonic fatigue.

Based on the following reasoning

- The risk of failing in fatigue is essentially the same as finding at least one inclusion with a critical combination of projected size and local stress within the volume

- The exact size of the inclusion is not important as long it is large enough

- The critically stressed volume is similar between samples

the ranking variable was defined as the size, S at which the acculumated density of inclusions represents a 50 % probability of finding a large inclusion within the sampled volume. From geometry and estimated stress distribution as well as the location of inclusions found in fatigue, the reference volume was chosen to be 300 mm^3 for the test specimens used.

In order to better model the behaviour of measured inclusion area densities, the estimated area distribution for each material was approximated by $N_A(z) = C_1 \exp(-C_2\sqrt{z})$.

The values of the ranking variables correlated with the fatigue strengths of the tested batches, see Fig. 7. Also, the ranking variables agreed well, with the exception of two
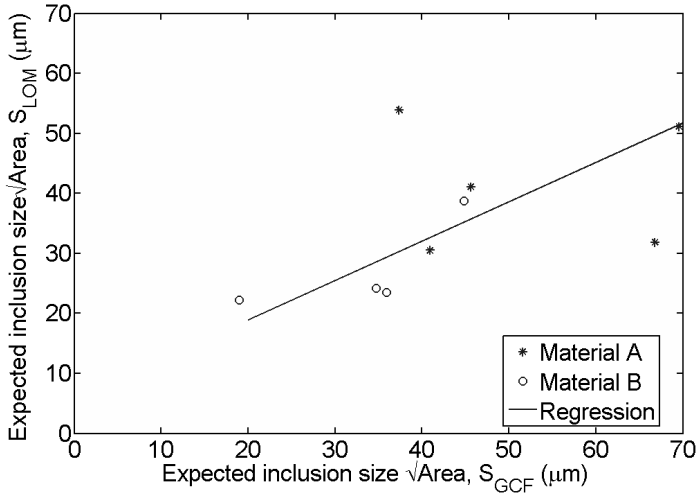

Figure 7: *Expected 50% inclusion sizes, $\sqrt{Area}$ (μm) from LOM measurements (S_{LOM}) and fractography results (S_{GCF}). In Paper II, material D is named "B".*

batches. In the first, defects other than inclusions acted as fatigue failure initiations. Those defects were not detected using the microscopy methods, resulting in a lower S_{GCF} value. In the other case, no inclusions were found in the largest size class using light optical microsope, giving a very low S_{LOM} value.

It was also found that for these materials the Gumbel distribution fits the fatigue initiating inclusions very well when all fatigue specimens are taken as one batch. The shape parameter of the extreme value distribution varied somewhat between batches, but was always within one standard deviation from 0.

This work is presented in paper II.

5.3   Different extreme value distributions

The extreme value distributions of fatigue initating defects in six different steel grades have been estimated. For the different steel grades, distinctly different values of the Generalized Extreme Value distribution shape parameter, ξ were found. For three of the materials ξ was found to be close to zero, approximating the GEV to special case of GEV mode I, or the Gumbel distribution, for which the largest expected inclusion size increases linearly with the logarithm of the amount of steel examined. In Fig. 8 the sizes of all found inclusions are seen, showing the difference of the location parameter for the three materials. The large uncertainty regarding the value of ξ for material E can also be observed. For two materials the values of ξ were found to be significantly positive, corresponding
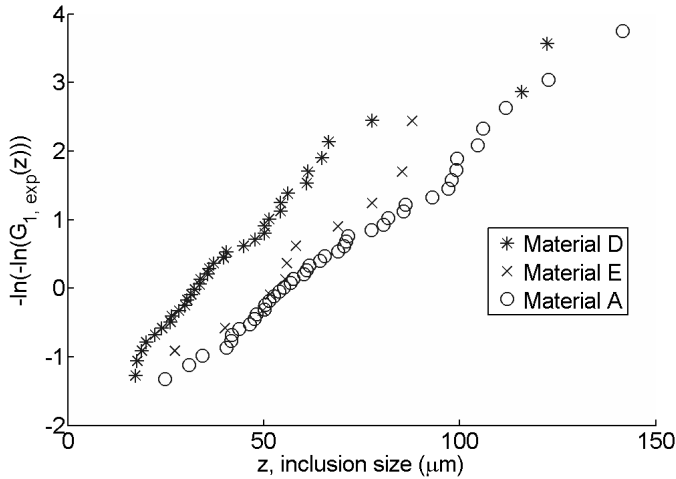

Figure 8: *Inclusion sizes for the three materials with $\xi = 0$. The similar values of σ mean that the main difference between the distributions is a shift due to the spread in μ. From Paper III.*

to underlying inclusion densities decaying slower than exponential with increasing size. Finally, for one material the estimated value of ξ is significantly negative, which corre-

sponds to a finite expected largest inclusion size. The sizes of inclusions found in these three material are shown in Fig. 9.
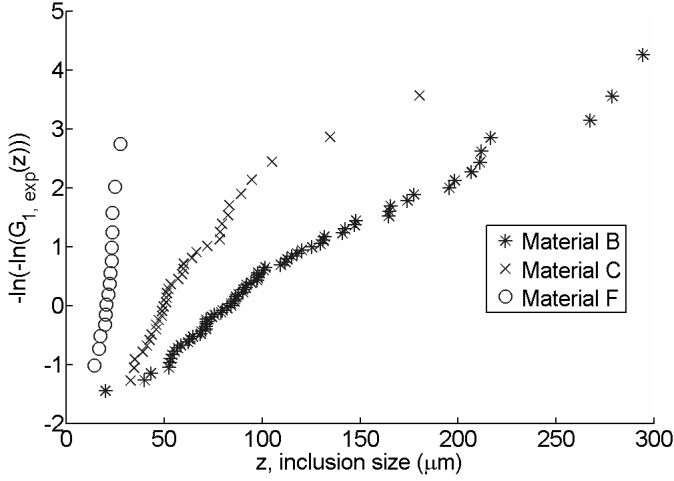

Figure 9: *Inclusion sizes for the three materials with $\xi \neq 0$. The heavier tail of material C is seen by the decreasing slope for larger inclusion sizes. From Paper III.*

These results are presented in paper III.

6   Discussion

The inclusions found in the tested steels are usually composed of several particles, often with differing chemical compositions within the different parts of the inclusion as seen in Fig. 10. A comparison between the predicted "safe size" according to the Murakami $\sqrt{Area}$ model and sizes of inclusions causing fatigue failure, illustrated in Fig. 11 shows a significant between the smallest inclusions found on fatigue fracture surfaces and the critical size. It is likely that not the whole area of the inclusion found is active during fatigue crack initiation. In Fig. 12 the fracture surface shows lines pointing to a part of the inclusion, about 30 μm in length, where the initiation is likely to have taken place.

The shape parameter ξ of the Generalized Extreme Value distribution varies between the tested batches and choosing one specific mode of the GEV should be done with caution. For materials A and D, the Gumbel (mode I) is chosen based on the distribution of all inclusions, treating all specimens as if they were taken from one batch, as seen in Fig. 8. For material C, the value of the shape parameter is positive for all individual batches as well as for the aggregated batch.

The detection of defects other than inclusions in very high cycle fatigue may can be problematic when measuring cleanliness. On the other hand, calculations of fatigue strength
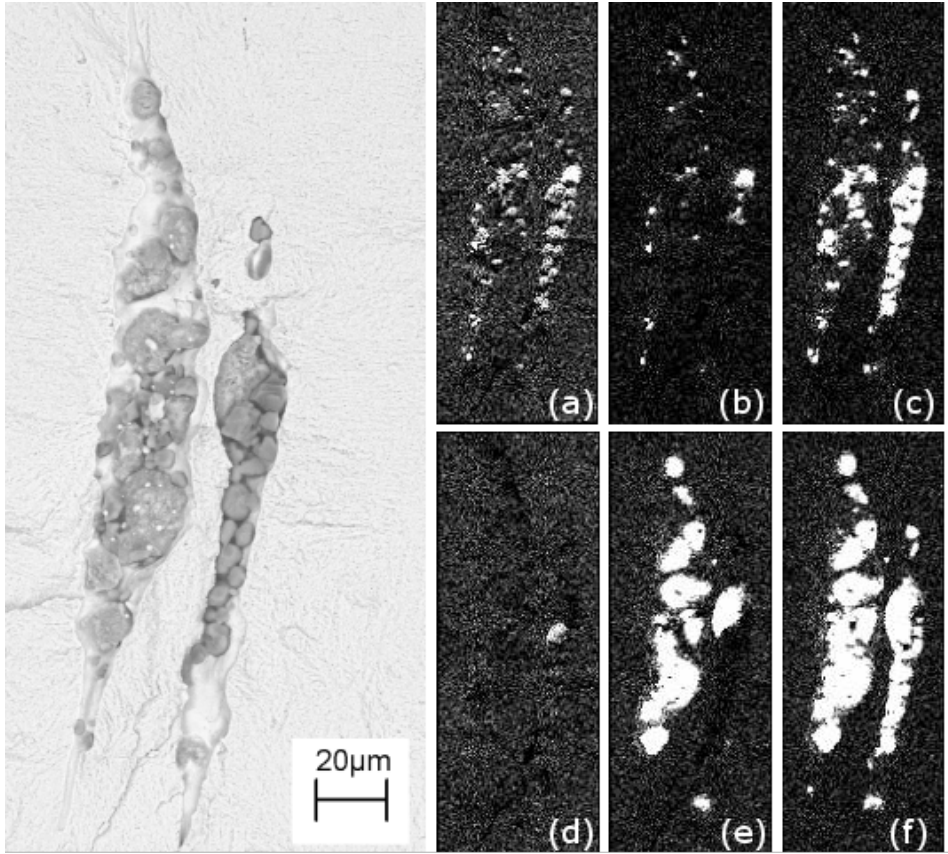
Figure 10: *Stringer-like inclusion found at fatigue initiation site. Left: Backscatter detector. Right: Chemical mapping obtained using EDS, (a) Oxygen, (b) Magnesium, (c) Aluminium, (d) Silicon, (e) Sulphur, (f) Calcium.*
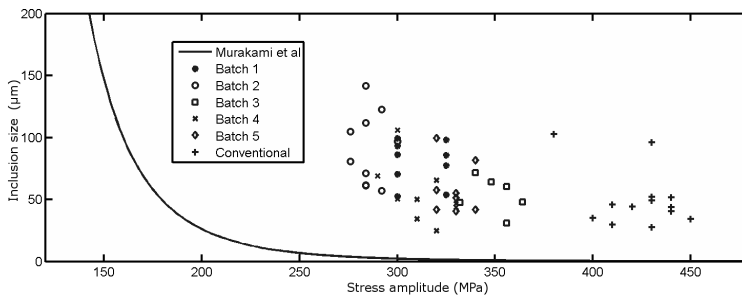

Figure 11: *Inclusion size ($\sqrt{Area}$ in μm) vs Fatigue stress amplitude (in MPa). Found inclusions are plotted at the nominal stress amplitude used during tests. From Paper I.*
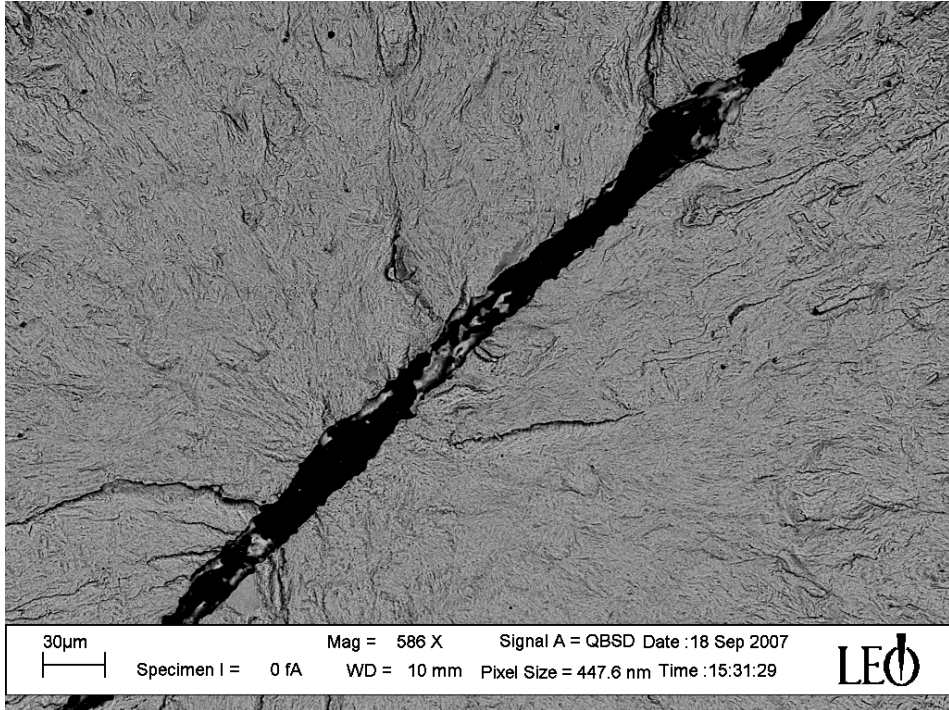
Figure 12: *Stringer inclusion at fatigue initiation point. Image contrast has been increased to show lines indicating the location of initiation within the inclusion.*

based on area scanning methods can be overly optimistic, failing to recognise competing fracture initiating defects.

7 Conclusions

Fatigue in the gigacycle regime is an effective way of finding large inclusions in highly clean steels. Most of the large inclusions found in the investigated materials contain several grains and show a distinct directionality along the working direction of the steel.

Fatigue to very high numbers of cycles can be used to estimate the distribution of large inclusions in steel using extreme value statistics.

A model for ranking materials based on their inclusion content is proposed, defined as the size S, at which the volume density predicts a 50% probability that a specific volume contains one inclusion of size S. The model is tested on nine batches from two materials and it is found that results from optical microscopy and fatigue fractography agree reasonably well.

Finding all three modes of the Generalized Extreme Value distribution (presented in Paper III) clearly shows that the assumption of Gumbel-distributed sizes must be confirmed for each new material. It is also shown that the shape parameter may differ considerably for materials produced by the same route.

8 Future work

- Include impact of uncertainties in the estimation of densities from Gumbel distribution

- Include goodness-of-fit tests for Generalized Extreme Value distribution approximation

- Find an analogue for the Gumbel $\rightarrow$ volume density calculation for non-Gumbel extreme value distributions

- Design a test procedure that uses ultrasonic resonance fatigue testing to provide reliable estimates of extreme value distribution of inclusions in a way that is possible to run at a per-batch basis during normal production.

References

[1] Mats Randelius. *Licentiate thesis: Influence of microstructure on fatigue and ductility properties of tool steels*. Licentiate thesis, KTH, 2008.

[2] G. P. Sendeckyj. *Early Railroad Accidents and the Origins of Research on Fatigue or Metals*, pages 472–492. Elsevier, Oxford, UK, 2006.

[3] C. R. Sohar, A. Betzwar-Kotas, C. Gierl, B. Weiss, and H. Danninger. Influence of surface residual stresses on gigacycle fatigue response of high chromium cold work tool steel. *Materialwissenschaft und Werkstofftechnik*, 39(3):248–257, 2008.

[4] Claude Bathias. There is no infinite fatigue life in metallic materials. *Fatigue & Fracture of Engineering Materials & Structures*, 22(7):559–565, 1999.

[5] Elisabeth Joossens. *Extreme value statistics : second-order models and applications in metal fatigue.* PhD thesis, K. U. Leuven, June 2006.

[6] Marcolino Fernandes, Noé Cheung, and Amauri Garcia. Investigation of nonmetallic inclusions in continuously cast carbon steel by dissolution of the ferritic matrix. *Materials Characterization*, 48:255–261, 2002.

[7] Hans Nordberg. Initiation of fatigue failures by non-metallic inclusions. In Nils-Gunnar Ohlson and Hans Nordberg, editors, *Classical Fatigue*, 1985.

[8] R. W. Hertzberg. *Deformation and Fracture Mechanics of Engineering Materials*. John Wiley & Sons, 3rd edition, 1996.

[9] M. Ciavarella and F. Monno. On the possible generalizations of the Kitagawa-Takahashi diagram and of the el haddad equation to finite life. *International Journal of Fatigue*, 28:1826–1837, 2006.

[10] J. J. Kruzic and R. O. Ritchie. Kitagawa-takahashi diagrams define the limiting conditions for cyclic fatigue failure in human dentin. *Journal of Biomedical Materials Research Part A*, 79A(3):747–751, 2006.

[11] Stuart Coles. *"Introduction to Statistical Modeling of Extreme Values"*. Springer-Verlag, 2001.

[12] Sara Lorén. Estimating inclusion distributions of hard metal using fatigue tests. *International Journal of Fatigue*, 25:129–137, 2005.

[13] C. W. Anderson, J. de Maré, and H. Rootzen. Methods for estimating the sizes of large inclusions in clean steels. *Acta Materialia*, 53:2295–2304, 2005.

Estimating inclusion content in high performance steels

Non-metallic inclusions in steel pose a major problem for the fatigue resistance, especially regarding fatigue at very long lives corresponding to low cyclic stress levels, as well as being detrimental to material toughness and polishability.

The largest inclusions are quite rare, which makes conventional detection methods time-consuming if reliable results are to be obtained. Based on surface scanning using light or electron microscopes, these methods provide results that have to be converted to reflect the statistical volume distribution of inclusions.

Very high cycle fatigue (in the order of 10^9 cycles or more) using ultrasonic fatigue at 20 kHz has been found efficient at finding the largest inclusions in volumes of about 300 mm³ per specimen. The inclusions found at the fatigue initiation site can then been used to estimate the distribution of large inclusions using extreme value statistics.

In this work, a new method for estimating the volume distribution of large inclusions is presented as well as a suggested ranking variable based on the volume distribution.

Results from fatigue fractography and area scanning methods are compared to the endurance limit at 10^9 cycles for a number of batches from two high performance steels.

In addition, the extreme value distributions of fatigue initiating inclusions in six high performace steels, produced by different routes, are presented. It is shown that all modes of the Generalized Extreme Values distribution can be found in different materials. This result shows that the assumption of mode I distribution, also known as Gumbel or Largest Extreme Value distribution, must be substantiated.